Published in final edited form as:
Mol Microbiol. 2014 May ; 92(3): 570–585. doi:10.1111/mmi.12576.

A 5′ UTR-mediated Translational Efficiency Mechanism Inhibits the *Candida albicans* Morphological Transition

Delma S. Childers[†], **Vasanthakrishna Mundodi**, **Mohua Banerjee**, and **David Kadosh**[*]
Department of Microbiology and Immunology, University of Texas Health Science Center at San Antonio, 7703 Floyd Curl Dr., MC: 7758, San Antonio, TX 78229-3900

SUMMARY

While virulence properties of *Candida albicans*, the most commonly isolated human fungal pathogen, are controlled by transcriptional and post-translational mechanisms, considerably little is known about the role of post-transcriptional, and particularly translational, mechanisms. We demonstrate that *UME6*, a key filament-specific transcriptional regulator whose expression level is sufficient to determine *C. albicans* morphology and promote virulence, has one of the longest 5′ untranslated regions (UTRs) identified in fungi to date, which is predicted to form a complex and extremely stable secondary structure. The 5′ UTR inhibits the ability of *UME6*, when expressed at constitutive high levels, to drive complete hyphal growth, but does not cause a reduction in *UME6* transcript. Deletion of the 5′ UTR increases *C. albicans* filamentation under a variety of conditions but does not affect *UME6* transcript level or induction kinetics. We show that the 5′ UTR functions to inhibit Ume6 protein expression under several filament-inducing conditions and specifically reduces association of the *UME6* transcript with polysomes. Overall, our findings suggest that translational efficiency mechanisms, known to regulate diverse biological processes in bacterial and viral pathogens as well as higher eukaryotes, have evolved to inhibit and fine-tune morphogenesis, a key virulence trait of many human fungal pathogens.

INTRODUCTION

Candida albicans is the major cause of human fungal disease worldwide. While normally a commensal in the mammalian host, this organism is responsible for a wide range of mucosal and systemic infections (Odds, 1988, Calderone & Clancy, 2012). Immunocompromised individuals, including cancer patients on chemotherapy, organ transplant recipients, and recipients of artificial joints and prosthetic devices, are particularly susceptible (Dupont, 1995, Weig *et al.*, 1998). *Candida* species are now the fourth-leading cause of hospital-acquired bloodstream infections in the U.S. with a ~40% mortality rate (Edmond *et al.*, 1999, Wisplinghoff *et al.*, 2004) and approximately $1 billion per year is spent in this country on antifungal therapies to treat systemic candidiasis (Miller *et al.*, 2001).

C. albicans is known to possess a number of properties which contribute to virulence, including the ability to undergo a reversible morphological transition from single oval-

[*]Corresponding author, Tel: (210) 567-3976, Fax: (210) 567-6612, kadosh@uthscsa.edu.
[†]Present address: Aberdeen Fungal Group, School of Medical Sciences, University of Aberdeen, Institute of Medical Sciences, Foresterhill, Aberdeen, United Kingdom

shaped yeast cells to pseudohyphal and hyphal filaments (elongated cells attached end-to-end) in response to specific environmental cues in the host environment (eg: serum and body temperature, 37°C) (Odds, 1988, Calderone & Clancy, 2012). Hyphal filaments are known to play an important role in tissue invasion, lysis of macrophages as well as evasion of the host immune system (Kumamoto & Vinces, 2005). Several key experiments have also indicated that the *C. albicans* yeast-filament transition is required for virulence in a mouse model of systemic candidiasis (Lo *et al.*, 1997, Saville *et al.*, 2003, Braun & Johnson, 1997). Additional virulence-related processes include adhesion to host epithelial and endothelial cells, secretion of degradative enzymes, phenotypic switching and the ability to form biofilms on host surfaces as well as implanted medical devices. Both phenotypic switching and biofilm formation can lead to the development of antifungal drug resistance (Hoyer *et al.*, 2008, Sundstrom, 1999, Calderone & Clancy, 2012, Douglas, 2002, Schaller *et al.*, 2005).

Given the importance of the virulence properties described above for *C. albicans* pathogenicity, intense research efforts have focused on elucidating molecular mechanisms by which they are controlled, particularly in response to host environmental cues. Thus far, considerable progress has been made towards the identification and characterization of post-translational mechanisms. Both mitogen-activated protein (MAP) kinase and Ras cAMP-protein kinase A (PKA) signaling pathways have been shown to mediate *C. albicans* filamentation in response to a variety of environmental cues including starvation, serum and glucose (Biswas *et al.*, 2007). Phosphorylation of septins and other targets by the Hgc1-Cdc28 cyclin/Cdk complex under filament-inducing conditions is important for the physical process of *C. albicans* hyphal development (Wang, 2009). Histone acetylation and/or deacetylation are also important for *C. albicans* stress adaptation, survival in macrophages, morphogenesis and phenotypic switching (Lopes da Rosa & Kaufman, 2012, Hnisz *et al.*, 2010, Lopes da Rosa *et al.*, 2010). In addition, ubiquitination and sumoylation have both been shown to control *C. albicans* morphogenesis, cell cycle progression and stress response (Leach *et al.*, 2011b, Leach *et al.*, 2011a, Leach & Brown, 2012).

Significant progress has also been made towards the identification of transcriptional mechanisms that control *C. albicans* virulence properties. A variety of transcriptional regulators of filamentous growth (eg: Efg1, Cph1, Nrg1) have been shown to function as downstream targets of the MAP kinase and/or Ras-cAMP-PKA signaling pathways described above (Biswas et al., 2007, Calderone & Clancy, 2012, Lu *et al.*, 2011). Many of these regulators control the expression of adhesins and secreted degradative enzymes (Felk *et al.*, 2002, Sohn *et al.*, 2003, Kadosh & Johnson, 2005). In addition, transcriptional regulatory mechanisms are known to control phenotypic switching, biofilm formation, stress response, iron acquisition and the development of antifungal drug resistance (Sellam *et al.*, 2012, Chen *et al.*, 2011, Zordan *et al.*, 2007, Nobile *et al.*, 2012, Sanglard *et al.*, 2009).

In contrast to post-translational and transcriptional mechanisms, considerably little is known about post-transcriptional mechanisms that control *C. albicans* virulence properties. A She3-dependent RNA transport system is important for both hyphal development and the transport of certain filament-specific transcripts to the hyphal tip (Elson *et al.*, 2009). A nuclear localization mechanism has recently been shown to control Sef1, a transcriptional regulator

important for virulence and iron uptake in the host (Chen & Noble, 2012). An mRNA stability mechanism is also known to regulate filamentation and virulence (Cleary *et al.*, 2012) and the Ccr4-Pop2 mRNA deadenylase complex controls cell wall integrity, filamentation and antifungal drug resistance (Dagley *et al.*, 2011, Tucker *et al.*, 2001, Chen *et al.*, 2001). Information regarding translational control of *C. albicans* virulence properties is particularly lacking. Interestingly, however, a recent whole-genome RNA-Seq analysis has revealed that several key transcripts encoding proteins involved in filamentation, biofilm formation, white-opaque phenotypic switching (important for mating), adhesion, degradation of host membrane proteins and other processes important for *C. albicans* pathogenesis have unusually long (> 500 bp) 5′ untranslated regions (UTRs) (Bruno *et al.*, 2010); similar results were found in an independent experiment using high-resolution *C. albicans* tiling arrays (Sellam *et al.*, 2010). Previous studies in other organisms have revealed that 5′ UTRs can play an important role reducing overall translational efficiency by a variety of mechanisms, including the formation of highly stable secondary structures which inhibit ribosome scanning and/or accessibility (Mignone *et al.*, 2002).

In this study, we identify an exceptionally long 5′ UTR and examine the role that this element plays in controlling the expression of *UME6*, which encodes a critical filament-specific transcriptional regulator of the *C. albicans* morphological transition. *UME6* is important for controlling the level and duration of filament-specific gene expression in response to filament-inducing conditions. Strains deleted for *UME6* are defective for hyphal extension and attenuated for virulence in a mouse model of systemic candidiasis (Banerjee *et al.*, 2008, Zeidler *et al.*, 2009) and a recent study has specifically demonstrated that Ume6 protein levels play a critical role in these processes (Lu *et al.*, 2013). We have also previously shown that expression levels of *UME6* are sufficient to sequentially specify *C. albicans* yeast, pseudohyphal and hyphal morphologies in a dosage-dependent manner (Carlisle *et al.*, 2009). Here, we demonstrate that the *UME6* 5′ UTR plays an important role in specifically inhibiting Ume6 protein expression, thus affecting the ability of this regulator to determine *C. albicans* morphology. We also specifically examine the role of this 5′ UTR in controlling *UME6* at the level of translational efficiency and provide new information about translational regulation of morphological transitions in pathogenic fungi.

RESULTS

Analysis of the *C. albicans UME6* upstream region identifies an unusually long 5′ UTR

Given the importance of *UME6* for *C. albicans* morphology determination and virulence, we initially sought to identify and characterize upstream regulatory elements that control expression of this transcription factor. We immediately noticed the presence of an unusually long intergenic region (20.6 kb) between *UME6* and the nearest upstream gene, *orf19.177*, on *C. albicans* chromosome 1 (Figure 1A). In order to identify upstream elements in the intergenic region important for *UME6* function, we first generated a *ume6Δ/+* strain in which one allele of the *UME6* coding sequence, along with 19.3 kb of upstream sequence, was deleted and replaced with a *HIS1* marker (this strain was phenotypically equivalent to a strain deleted for one copy of only the *UME6* open reading frame). Next, a variety of deletions of varying lengths were generated in the upstream intergenic region of the second

UME6 allele. Morphology phenotypes of all deletion strains, along with *ume6*Δ/+ and *ume6*Δ/Δ control strains, were compared on solid medium in the presence of serum at 37°C, a strong filament-inducing condition (Figure 1B). Consistent with previous observations (Banerjee et al., 2008), the *ume6*Δ/Δ mutant was significantly defective for filamentation relative to the *ume6*Δ/+ strain. We observed that deletion strains containing only 4 kb and 5 kb of the upstream *UME6* intergenic region showed a filamentation defect equivalent to that of the *ume6*Δ/Δ mutant. In contrast, strains containing 6 kb or greater of the *UME6* upstream region showed a level of filamentation similar to that of the *ume6*Δ/+ parent strain. These results indicate that at least 6 kb of the upstream region is required for *UME6* function with respect to filamentation and suggest that critical promoter elements are located in this region. In order to test this hypothesis, a *C. albicans* strain was generated in which the 6 kb *UME6* upstream region was placed upstream of a heterologous *Streptomyces thermophilus lacZ* reporter gene. As shown in Figure 1C, the 6 kb *UME6* upstream region was sufficient to drive ~25-fold transcriptional induction of the *lacZ* reporter in the presence of serum at 37°C vs. 30°C only. In contrast, the *lacZ* reporter alone did not show significant induction. These results indicate that the 6 kb *UME6* upstream region contains important promoter elements and suggest that deletion strains containing only 5 kb and 4 kb of upstream sequence are defective for filamentation because they lack these elements. In order to map the transcriptional initiation site within this region, we performed a 5′ RACE (rapid amplification of cDNA ends) analysis using cDNA prepared from wild-type cells grown in the presence of serum at 37°C. This analysis revealed the presence of three transcript start sites located at positions −3041 bp, −2126 bp and −1923 bp relative to the translational initiation codon (+1) (Figures 1D and S1). These findings are consistent with a previous report which, using RNA-Seq analysis, indicated that the *UME6* 5′ UTR is greater than 1500 bp in length (Bruno et al., 2010). Based on the total size of the *UME6* transcript, as determined by Northern analysis, as well as known sizes of *UME6* open reading frame and 3′ UTR (Braun *et al.*, 2005, Bruno et al., 2010), the major transcription start site is located at 3041 bp upstream of the *UME6* start codon. *UME6* transcripts whose sizes are consistent with 2.1 kb and 1.9 kb transcription start sites were not detected by Northern analysis, suggesting that these are minor start sites. The 3041 bp 5′ UTR of *UME6* is much longer than the average 5′ UTR (~150 bp, based on our calculations) in *C. albicans* (Bruno et al., 2010) and, based on a search of the UTRdb database (Grillo *et al.*, 2010), is one of the longest 5′ UTRs identified in fungi to date.

An *in silico* analysis of the *UME6* 5′ UTR sequence revealed the presence of two upstream open reading frames (uORFs) which are 39 bp and 102 bp in length and located at −1519 bp and −685 bp, respectively, upstream from the *UME6* start codon (Figure 1D). In order to perform a predicted structure analysis of the *UME6* transcript we used the RNA folding program mFold (http://mfold.rna.albany.edu/?q=mfold/) (Zuker, 2003). This program is widely used and was selected because it performs calculations based on Minimum Folding Energy (MFE) algorithms, which are typically more accurate in determining major substructures of RNAs with low folding energies. As indicated in Figure 2, an mFold analysis of the full-length *UME6* transcript sequence predicted that the 5′ UTR forms a complex secondary structure. The 5′ UTR alone is predicted to be extremely stable with a very low folding free energy (ΔG) of −468.1 kcal/mol; the full-length *UME6* transcript has a

predicted ΔG of −1017.7 kcal/mol. An independent analysis using RNAFold (http://rna.tbi.univie.ac.at/cgi-bin/RNAfold.cgi) (Zuker & Stiegler, 1981), a different MFE-based RNA structural prediction program, predicted similar structures and folding energies. The average folding free energy for 5′ UTRs of transcripts encoding transcription factors, growth factors, receptors and other regulatory proteins across species is −50 kcal/mol (Davuluri *et al.*, 2000). Both uORFs and stable secondary structures are characteristic of 5′ UTRs which are known to play important roles in translational regulation (Mignone et al., 2002) and their apparent presence in this 5′ UTR suggested that *UME6* may be controlled by such a mechanism.

Deletion of the *UME6* 5′ UTR increases *C. albicans* filamentous growth but does not affect *UME6* transcript level or induction kinetics

In order to determine whether the long 5′ UTR was important for the ability of *UME6* to control *C. albicans* filamentous growth, we generated a strain in which both copies of the *UME6* 5′ UTR were deleted. The 5′ UTR deletion spanned from positions −3011 bp to −47 bp upstream of the *UME6* start codon and this sequence was replaced with a 34 bp *FRT* site as well as XhoI and NotI restriction sites (see Supporting Information for details as well as a complete sequence of the fusion joint). Importantly, the complete *UME6* open reading frame (ORF), as well as 46 bp immediately upstream of the *UME6* AUG start codon, were left intact. As shown in Figure 3A, the *UME6 5′ utr*Δ/Δ strain showed a mild increase in filamentation, relative to that of the wild-type control strain, when cells were grown on solid YEPD medium in the presence of serum at 37°C. The increased filamentous growth phenotype of the *UME6 5′ utr*Δ/Δ mutant was more pronounced on solid Spider (nitrogen and carbon starvation) and Lee's pH 6.8 media, but was not observed when cells were grown on solid YEPD medium at 30°C for 3 days (non-filament-inducing conditions). The *UME6 5′ utr*Δ/Δ mutant also showed greater filamentation than that of a wild-type control strain in liquid Spider medium at 37°C (data not shown). These results indicate that the *UME6* 5′ UTR functions to inhibit *C. albicans* filamentation in response to a variety of filament-inducing conditions.

Many UTRs (primarily 3′ UTRs) are known to control the level of their respective transcripts (Mignone et al., 2002). In order to determine whether the *UME6* 5′ UTR plays a role in controlling *UME6* transcript level and/or induction kinetics, a serum and temperature-induction time course experiment was carried out using both *UME6 5′ utr*Δ/Δ and wild-type control strains. Cells from each strain were harvested at the zero time point, as well as various post-induction time points, and total RNA was prepared for Northern analysis. As shown in Figure 3B, *UME6* induction kinetics, as well as overall transcript level, in the *UME6 5′ utr*Δ/Δ strain appeared nearly identical to those observed in the wild-type control strain. We have also observed that both of these strains express *UME6* at an equivalent level when cells are grown in Spider medium at 37°C (Figure S2).

The *UME6* 5′ UTR inhibits the ability of *UME6*, when expressed at constitutive high levels, to drive complete hyphal growth but does not cause a reduction in *UME6* transcript

We have previously demonstrated that constitutive high-level expression of *UME6* is sufficient to drive nearly complete hyphal growth of *C. albicans* in the absence of filament-

inducing conditions (Carlisle et al., 2009). This result was obtained using a strain in which the *E. coli tet* operator (*tetO*) was placed upstream of the start codon for one allele of *UME6* (the 5′ UTR was not present). In the absence of doxycycline (Dox, a tetracycline derivative), a transactivator binds *tetO* and *UME6* is expressed at high constitutive levels; in the presence of Dox, the *UME6* allele is shut off. When the *tetO-UME6* strain is initially grown in the presence of Dox and then transferred to medium lacking Dox, *C. albicans* cells sequentially transition from yeast to pseudohyphae to a nearly complete hyphal population over a time course in the absence of filament-inducing conditions. In order to determine the effect of the *UME6* 5′ UTR on the ability of *UME6* levels to specify *C. albicans* morphology, a similar strain was generated in which the *tet* operator was placed immediately upstream of the 3 kb 5′ UTR. Both *tetO-5′UTR-UME6* and *tetO-UME6* strains were grown under non-filament-inducing conditions in the presence of Dox, and then cultures were diluted into medium lacking Dox, as described above. As a control, cultures from both strains were also diluted into medium containing Dox. Cell morphology of both strains was examined at various time points following Dox depletion. By the 3 hour time point, the *tetO-5′UTR-UME6* strain grew as pseudohyphae (Figure 4A). We also observed that this strain showed a higher proportion of yeast cells (32%) compared to that of the *tetO-UME6* strain (14%). By the 10 hour time point, the *tetO-UME6* strain had transitioned to a nearly complete hyphal population (note: in our previous study (Carlisle et al., 2009) this transition was completed within 9 hours, most likely due to differences in culture volume) whereas the *tetO-5′UTR-UME6* strain grew as a mixture of yeast, pseudohyphae and hyphae. Even following growth overnight in the absence of Dox, the *tetO-5′UTR-UME6* strain showed a mixed population of cell morphologies and was unable to transition completely to hyphae (Figure S3). Also, consistent with previous observations (Carlisle et al., 2009, Carlisle & Kadosh, 2010), control cells of both strains grown in the presence of Dox remained in the yeast morphology (data not shown). Overall, these results indicate that the 5′ UTR is important for the ability of *UME6* expression levels to specify *C. albicans* morphology.

In order to examine whether the 5′ UTR affects *C. albicans* morphology determination by causing a reduction in *UME6* transcript levels, total RNA was prepared from cells of both *tetO-5′UTR-UME6* and *tetO-UME6* strains at each time point of the time course experiment described above and used for quantitative RT-PCR analysis. As shown in Figure 4B, in the *tetO-UME6* strain the *UME6* transcript was induced 8.7-fold at the 1-hour time point following Dox depletion and remained induced at a high level (12- to 19-fold) from the 2-hour time point through the remainder of the time course. *UME6* was expressed at roughly equivalent levels in both the *tetO-5′UTR-UME6* and *tetO-UME6* strains at the 1 hour time point in the absence of Dox. Interestingly, over the remaining time points in the absence of Dox, *UME6* levels in the *tetO-5′UTR-UME6* strain were consistently higher (38- to 54-fold induced) than those of the *tetO-UME6* strain. As expected, *UME6* was not expressed to a significant degree in either strain when cells were grown in the presence of Dox. Overall, these results clearly indicate that the inability of the *tetO-5′UTR-UME6* strain to drive complete hyphal growth in the absence of Dox cannot be attributed to a reduction in *UME6* transcript levels.

The *UME6* 5′ UTR functions to inhibit translational efficiency of *UME6*

Given the failure of the 5′ UTR to cause a reduction in *UME6* transcript level or control *UME6* induction kinetics, we hypothesized that this region may control the translational efficiency of *UME6*. This hypothesis was supported by previous reports documenting the role of 5′ UTR regions in translational regulation, as well as our observation that the *UME6* 5′ UTR is predicted to possess a highly stable secondary structure and contains two uORFs, all of which have been associated with translational control in prior studies (Pickering & Willis, 2005, Mignone et al., 2002). In order to test this hypothesis, we performed a polysome profiling assay. Wild-type and *UME6 5′ utr*Δ/Δ strains showed similar polysome profiles when cells were grown under filament-inducing (serum at 37°C) and non-filament-inducing (30°C) conditions (Figure 5A). In addition, treatment with EDTA, a known inhibitor of polysome formation, disrupted the polysome profile in both strains, as expected. As indicated in Figure 5B, the *UME6* transcript generally showed significantly greater association with the polysome fractions of the *UME6 5′ utr*Δ/Δ vs. wild-type control strain when cells were induced by serum at 37°C. The greatest differences in association (~ 10-fold) were observed in the final fractions (10 and 11), which are richest in polysomes. The *UME6* transcript of the wild-type strain generally showed a similar abundance, regardless of whether qRT-PCR primers for the open reading frame or 5′ UTR were used for detection, indicating that the 5′ UTR was still present. In addition, an *ACT1* control transcript generally did not show large differences in abundance between the wild-type and *UME6 5′ utr*Δ/Δ strains (Figure S4). As expected, we also observed an overall shift in transcript abundance from polysome-bound to unbound fractions upon treatment with EDTA (data not shown). Also consistent with previous observations that *UME6* is transcriptionally induced in a filament-specific manner (Banerjee et al., 2008, Zeidler et al., 2009), very low levels of *UME6* transcript were observed in all fractions when cells of both wild-type and *UME6 5′ utr*Δ/Δ strains were grown under non-filament-inducing conditions (30°C) (Figure 5B). These results strongly suggest that the 5′ UTR functions to inhibit *UME6* translational efficiency by reducing association of the *UME6* transcript with polysomes under filament-inducing conditions.

In order to confirm that the *UME6* 5′ UTR functions to inhibit Ume6 protein expression, the 5′ UTR was deleted in a strain expressing Myc-tagged Ume6 and cells were induced to form filaments by growth at 37°C in the presence of serum. As shown in Figure 6A, Ume6-Myc showed a significantly greater induction in the *5′ utr*Δ-*UME6-MYC* strain compared to that observed in the *UME6-MYC* control strain. We also observed increased expression of Ume6-Myc in the *5′ utr*Δ-*UME6-MYC* vs. *UME6 MYC* strain in the presence other filament-inducing conditions, including 37°C only, Spider at 37°C and Lee's pH 6.8 media (Figures 6A and 6B). Interestingly, the extent to which Ume6 levels rose upon deletion of the 5′ UTR appeared to vary between filament-inducing conditions (eg: compare 37°C + Spider and Lee's pH 6.8). These differences were reproducible based on multiple replicates (two replicates for 37°C and 37°C + Serum and three replicates for 37°C + Spider and Lee's pH 6.8), suggesting that translational inhibition by the 5′ UTR may, to some degree, be modulated by environmental signals which control *C. albicans* filamentation. A Northern analysis indicated that for all filament-inducing conditions there was not a significant difference in the *UME6* transcript level in *UME6 MYC* vs. *5′ utr*Δ-*UME6-MYC* strains

(Figure S5). As expected, *UME6* levels were generally higher in the strongest filament-inducing condition, serum at 37°C, compared to those observed in Spider at 37°C, Lee's pH 6.8 and 37°C only, which are weaker inducing conditions. Overall, these findings suggest that reduced translational efficiency directed by the *UME6* 5′ UTR results in a significant decrease in Ume6 protein expression in the presence of a variety of filament-inducing conditions.

To determine whether the *UME6* 5′ UTR was sufficient to inhibit translation, we placed the 5′ UTR immediately upstream of a heterologous *GFP*γ reporter gene driven by a constitutive *ACT1* promoter. *ACT1*$_{pr}$-*UME6 5′ UTR-GFP* and *ACT1*$_{pr}$-*GFP* strains were grown under non-filament inducing conditions and GFP protein expression was quantified by fluorometry. As shown in Figures 7A and S6, the 5′ UTR caused a significant reduction in GFP protein levels. Indeed, the *ACT1*$_{pr}$-*UME6 5′ UTR- GFP* strain showed fluorescence values equivalent to those of a wild-type control strain which does not express GFP. In addition, removal of both uORFs did not affect the ability of the *UME6* 5′ UTR to inhibit GFP protein expression. Importantly, the ratio of GFP protein to transcript (as determined by qRT-PCR) was significantly higher in the *ACT1*$_{pr}$- *GFP* strain when compared to that of the *ACT1*$_{pr}$-*UME6 5′ UTR-GFP* and *ACT1*$_{pr}$-*UME6 5′ UTR uorf1*Δ *uorf2*Δ-*GFP* strains (Figure 7B). A Northern analysis also confirmed that the *GFP* transcript was expressed at equivalent levels in all three of these strains and not expressed in a wild-type control strain (Figure S7). These results strongly suggest that the *UME6* 5′ UTR is sufficient to inhibit translation, but not transcription, via a uORF-independent mechanism when placed in the context of a heterologous promoter.

DISCUSSION

In *C. albicans*, the most commonly isolated human fungal pathogen, a variety of post-translational and/or transcriptional mechanisms are known to be involved in the regulation of morphogenesis, adhesion, secretion of degradative enzymes, biofilm formation, phenotypic switching and other virulence properties. However, significantly less is known about post-transcriptional, and especially translational, mechanisms that control these processes (although several genes are known to be translationally regulated during filamentation in the non-pathogenic model yeast *Saccharomyces cerevisiae* (Park *et al.*, 2006)). Here, we describe a 5′ UTR-mediated translational efficiency mechanism that plays an important role in inhibiting *C. albicans* morphogenesis by controlling the expression of Ume6, a key filament-specific transcription factor. We provide several lines of evidence to support this mechanism: 1) deletion of the *UME6* 5′ UTR causes increased filamentation and hyphal growth but does not affect the induction kinetics or level of the *UME6* transcript, 2) the 5′ UTR inhibits the ability of *UME6*, when expressed at constitutive high levels, to drive complete hyphal formation but does not cause a reduction in *UME6* transcript, 3) the 5′ UTR specifically inhibits the ability of the *UME6* transcript to associate with polysomes and also inhibits Ume6 protein expression in the presence of a variety of filament-inducing conditions, 4) the *UME6* 5′ UTR is sufficient to inhibit translation, but not transcription, of a heterologous reporter gene. In addition, the *UME6* 5′ UTR is exceptionally long and contains several features which have previously been associated with translational control (Mignone et al., 2002, Pickering & Willis, 2005).

How exactly does the 5′ UTR function to inhibit translational efficiency of *UME6*? Based on previous studies (Mignone et al., 2002, Pickering & Willis, 2005), four possible mechanisms may explain our observations. First, as indicated by our *in silico* analysis, the *UME6* 5′ UTR contains two putative uORFs. Because, in eukaryotes, the small ribosomal subunit typically initiates translation at the first scanned AUG codon, the large majority of translation in the 5′ UTR may be initiating at the uORFs, rather than at the *UME6* start codon, depending on the context of ribosome capture. In this case, translation of *UME6* would occur as a result of either leaky ribosome scanning or re-initiation. However, our observation that removal of both uORFs does not significantly affect the ability of the *UME6* 5′ UTR to inhibit translation appears to exclude this mechanism.

A second mechanism by which the 5′ UTR may control *UME6* translational efficiency is by forming an extremely stable secondary structure (Figure 8). Stable 5′ UTR secondary structures have previously been shown to inhibit the ability of ribosomes to access and/or efficiently scan mRNA transcripts and reach the start codon (Mignone et al., 2002, Pickering & Willis, 2005). This mechanism is supported by our *in silico* analysis indicating the *UME6* 5′ UTR is predicted to form a complex and highly stable secondary structure with very low folding free energy. The predicted free energy of the 5′ UTR is about 9 times the free energy required for hairpin structures to block ribosome scanning (−50 kcal/mol) (Pelletier & Sonenberg, 1985, Kozak, 1989). Unfortunately, due to the exceptionally large size and predicted complexity of the *UME6* 5′ UTR, standard approaches (eg: compensatory base change and chemical probing experiments) to determine directly whether its secondary structure is important for controlling translational efficiency are not feasible. A deletion series analysis of the 5′ UTR suggested the possible involvement of certain regions in translational control, but was generally difficult to interpret since many of the partial deletion mutants also showed alterations in transcript levels when compared to those observed in *UME6-MYC* and *UME6-5′utr*Δ*-MYC* strains (data not shown). In addition, partial deletions in the 5′ UTR caused significant changes in predicted overall secondary structure, which further complicated the analysis and made it difficult to determine the role of specific native 5′ UTR structures in translational control.

A third mechanism involves *trans*-acting RNA-binding proteins, which may bind to specific structural or sequence elements located within the *UME6* 5′ UTR. These factors can compete with ribosomes for access to the transcript or induce secondary structures which inhibit ribosome scanning (Figure 8) (Adeli, 2011). Another related possibility is that the *UME6* 5′UTR functions to prevent the formation of an internal ribosomal entry site (IRES) which allows ribosomes to directly enter the transcript at the start codon, instead of scanning from the 5′ end. However, IRES elements have typically been identified in viral and mammalian, rather than yeast, mRNAs (Kozak, 2001, Mignone et al., 2002, Pickering & Willis, 2005).

A fourth mechanism for *UME6* 5′ UTR-mediated translational inhibition may involve alternative mRNA localization (Figure 8). 5′ UTRs have been shown to affect the subcellular localization of their respective transcripts and *C. albicans* is known to transport certain mRNAs in a She3-dependent manner to the apical tip of hyphal filaments (Mignone et al., 2002, Elson et al., 2009). P-bodies, known to be important for mRNA degradation and

storage, have recently been shown to accumulate during *C. albicans* hyphal development (Jung & Kim, 2011). Localization of the *UME6* transcript to a P-body or other cellular compartment could therefore possibly lead to restricted translation at specific subcellular locations or storage for translation at a later time. The RNA predicted structural analysis, in combination with our demonstration that the 5′ UTR inhibits association of *UME6* mRNA with polysomes, strongly suggests that the secondary structure and/or RNA-binding protein mechanisms play an important role. Importantly, the mechanisms described above are not mutually exclusive and could act either alone, in combination, or in conjunction with alternative mechanisms, to control the translational efficiency of *UME6*.

In many eukaryotic systems, post-transcriptional control mechanisms play an important role in rapidly fine-tuning the expression of genes involved in important developmental processes and the mechanism we have described here appears to be no exception. *UME6* encodes a key filament-specific transcriptional regulator which controls *C. albicans* morphology and virulence, as well as the level and duration of filament-specific gene expression. *UME6* also serves as an important downstream target for multiple filamentous growth signaling pathways and we have previously shown that the morphology of *C. albicans* cells is exquisitely sensitive to *UME6* transcript levels (Banerjee et al., 2008, Carlisle et al., 2009, Zeidler et al., 2009). Our observations that the *UME6 5′ utr*Δ/Δ strain shows a generally mild increase in filamentation only in the presence of filament-inducing conditions and that constitutive high-level expression of *UME6* in the presence of the 5′ UTR generates a mixed population of cell morphologies (rather than all yeast) suggest that the 5′ UTR-mediated translational efficiency mechanism serves to rapidly control and fine-tune Ume6 expression levels. Consistent with this observation, we have found that the level of translational inhibition directed by the *UME6* 5′ UTR can vary in the presence of different filament-inducing conditions, suggesting that translation of Ume6 can be modulated by environmental signals. Because *UME6* transcript levels are very low in non-filament-inducing conditions, it was not possible to determine whether the 5′ UTR affects *UME6* translation under these conditions. However, our *GFP* reporter experiment does suggest that the 5′ UTR can inhibit translation under non-filament-inducing conditions as well. A recent report has indicated that stabilization of Ume6 protein by multiple filamentous growth signaling pathways is critical for *C. albicans* hyphal development and maintenance (Lu et al., 2013). In this respect, the 5′ UTR-mediated translational inhibition mechanism may serve to rapidly reduce Ume6 protein levels, thus preventing unnecessary hyphal growth until appropriate host environmental cues are present.

Our results also suggest that the 5′ UTR may possess elements that can increase *UME6* mRNA levels, at least when *UME6* is expressed from a heterologous *tet* operator under non-filament-inducing conditions. Consistent with this observation, a recent report indicates that Ume6 can bind to its own upstream region in the vicinity of the 5′ UTR to increase transcription in a positive feedback loop (Lu et al., 2013). In addition, a transcription factor important for temperature-induced *C. albicans* morphogenesis, Hms1, has recently been shown to bind the *UME6* 5′ UTR and induce *UME6* expression (Shapiro *et al.*, 2012). Our finding that natural *UME6* transcript levels are not altered upon deletion of the 5′ UTR is most likely explained by the observation that a significant number of additional

transcriptional regulators appear to play an important role in the activation of *UME6* (likely via the promoter) under filament-inducing conditions (Zeidler et al., 2009). Alternatively, changes in chromatin structure resulting from introduction of the 5′ UTR in the context of the *tetO* cassette could possibly account for increased *UME6* transcript levels in the *tetO-5′ UTR-UME6* vs. *tetO-UME6* strain. Given the importance of Ume6 for determining morphology and controlling filament- and virulence-specific gene expression, it is not surprising that *C. albicans* has evolved multiple mechanisms (transcriptional, translational and post-translational) to carefully adjust the levels of this regulator under a variety of different environmental conditions.

Interestingly, a recent whole-genome RNA-Seq analysis has indicated that, similar to *UME6*, a significant number of *C. albicans* genes involved in a wide variety of processes important for pathogenicity possess unusually long (> 500 bp) 5′ UTRs (Bruno et al., 2010). Many of these genes encode transcriptional regulators that control filamentous growth, biofilm formation, white-opaque switching and/or antifungal drug resistance (eg: *EFG1*, *CPH1*, *RFG1*, *CZF1*, *FKH2*, *SFL1*, *CRZ1*, *UPC2*, *GCN4*, *SIR2*) (Stoldt *et al.*, 1997, Ramage *et al.*, 2002, Sonneborn *et al.*, 1999, Liu *et al.*, 1994, Kadosh & Johnson, 2001, Brown *et al.*, 1999, Vinces & Kumamoto, 2007, Zordan et al., 2007, Bensen *et al.*, 2002, Li *et al.*, 2007, Onyewu *et al.*, 2004, Santos & de Larrinoa, 2005, Silver *et al.*, 2004, Tripathi *et al.*, 2002, Perez-Martin *et al.*, 1999). Several genes encoding adhesins of the α-agglutinin-like (ALS) family (*ALS4*, *ALS5*, *ALS9*), which are important for interaction of *C. albicans* with host cells (Hoyer, 2001), secreted aspartyl proteases (*SAP1*, *SAP2*) and lipases (*LIP4*, *LIP8*) , important for the ability of *C. albicans* to degrade host cell membranes (Schaller *et al.*, 2003, Hube *et al.*, 2000), a superoxide dismutase (*SOD4*) involved in responding to oxidative stress in the host (Martchenko *et al.*, 2004, Frohner *et al.*, 2009), and a key regulator of iron-uptake genes and gastrointestinal commensalism (*SFU1*) (Chen et al., 2011) also have long 5′ UTRs. Finally, several genes that play critical roles in the mechanics of *C. albicans* hyphal development (*HGC1*, *CDC24*, *RGA2*) and cell cycle control (*CLN3*, *CLB4*) fall in this category as well (Zheng *et al.*, 2004, Zheng *et al.*, 2007, Bassilana *et al.*, 2003, Chapa y Lazo *et al.*, 2005, Bensen *et al.*, 2005, Bachewich & Whiteway, 2005, Wang, 2009). While not all of these genes may necessarily be controlled by a translational efficiency mechanism, the presence of a long 5′ UTR upstream of so many genes involved in virulence-related processes suggests, based on our findings, that this mechanism may play a significant role in controlling and fine-tuning *C. albicans* pathogenicity in the host.

There is also evidence to suggest that 5′ UTR-mediated translational efficiency mechanisms may play an evolutionarily conserved role in the regulation of morphogenesis and pathogenicity in non-*albicans Candida* species. Many of these species possess *UME6* orthologs and the synteny of the long upstream intergenic region is conserved in *Candida dubliniensis*, *Candida tropicalis*, *Candida parapsilosis*, *Candida guilliermondii* and *Candida lusitaniae* (*Candida* Gene Order Browser, http://cgob.ucd.ie/), but has diverged in the non-pathogenic model yeast *S. cereviseae*. In addition, a recent whole-genome RNA-Seq experiment has identified over 250 *C. parapsilosis* genes with 5′ UTRs greater than 500 bp in length, many of which appear to be involved in filamentous growth and pathogenicity

(Guida *et al.*, 2011) and several of which encode orthologs of the *C. albicans* genes with long 5′ UTRs discussed above (including *UME6*).

In bacterial and viral pathogens, 5′ UTR-mediated translational efficiency mechanisms have been shown to control a variety of biological processes, several of which are important for virulence. In *Listeria monocytogenes*, 5′ UTRs are important for controlling the translation of key virulence factors involved in the production of listeriolysin O (Johansson *et al.*, 2002, Wong *et al.*, 2004, Shen & Higgins, 2005). The *Haemophilus influenzae sxy* gene, which encodes an important regulator of DNA uptake, is also known to be translationally regulated by a 5′ UTR which forms an inhibitory secondary structure (Cameron *et al.*, 2008). In several viral pathogens, including poliovirus and Hepatitis C virus, 5′ UTRs contain IRES sequences important for controlling translational efficiency and viral replication (Balvay *et al.*, 2009). In higher eukaryotes, UTRs are known to mediate translational control of a wide variety of genes that function in diverse cellular processes, including cell cycle, stress response, oncogenesis, fertilization and development (Pickering & Willis, 2005, Chatterjee & Pal, 2009). 5′ UTRs have also been shown to affect the expression of genes associated with a number of human diseases including breast cancer, Alzheimer's disease, and bipolar affective disorder (BPAD) (Chatterjee & Pal, 2009). Our findings are significant because they suggest that in the major human fungal pathogen *C. albicans*, a 5′ UTR-mediated translational efficiency mechanism has evolved to inhibit and fine-tune morphogenesis, a key developmental process important for pathogenicity in the host environment.

Given that 5′ UTRs are likely to control the expression of a variety of important regulators of *C. albicans* morphology and/or virulence, what mechanisms are responsible for mediating translational control? How exactly do translational mechanisms modulate and/or fine-tune the expression of key virulence factors in response to host environmental conditions? Do certain components of the translation machinery respond to specific environmental cues? Is there crosstalk between translational mechanisms and known transcriptional and post-translational mechanisms which have previously been shown to control virulence properties? How and why did translational mechanisms apparently evolve to control so many genes associated with fungal pathogenicity? It is hoped that future research in this area will help to address these questions and shed more light on the important, but poorly understood, role that translational mechanisms may play in controlling a variety of processes important for fungal pathogenesis.

MATERIALS AND METHODS

Strains and DNA Constructions

A complete listing of strains used in this study is shown in Table S1. A detailed description of the plasmids and methods used to generate additional strains is provided in the Supplemental Materials and Methods section. All primers used for plasmid and strain constructions are described in Table S2.

Media and Growth Conditions

Standard non-filament-inducing growth conditions were YEPD (yeast extract-peptonedextrose) medium at 30°C. Induction of filamentous growth by 10% serum at 37°C was performed as described previously (Banerjee et al., 2008). Spider and Lee's media were prepared as previously described (Lee *et al.*, 1975, Liu et al., 1994). Induction of filamentous growth in Spider medium at 37°C was performed by first growing strains overnight in YEPD medium at 30°C. Cells were then washed and resuspended in 10 mL YEPD medium or Spider medium at a concentration of 1×10^6 cells mL^{-1}. 10 μL of cells from each suspension were inoculated into 50 mL pre-warmed YEPD medium at 30°C or Spider medium at 37°C, respectively. Cultures were grown for 36 hours and cells were harvested for RNA extraction and microscopic analysis. DK318 was used as the wild-type control for the filament induction and polysome profiling experiments. The *C. albicans* morphological transition time course experiment was performed by initially growing *tetO-UME6* and *tetO-5′UTR-UME6* strains overnight at 30°C in YEPD medium + 1.0 μg mL^{-1} Dox to OD_{600} ~ 0.5. 50 mL aliquots of cells from each strain were next washed once in prewarmed YEPD medium at 30°C and used to inoculate 1.5 L of YEPD medium in the presence or absence of 1.0 μg/mL Dox. Cultures were grown at 30°C and cells were harvested for RNA extraction at each hour for 10 hours. Cells for the zero hour time point were collected from the *tetO-UME6* overnight culture just prior to washing. For the 5′ RACE analysis, cells were induced with serum at 37°C as described previously (Banerjee et al., 2008) and harvested at 30 min. (for identification of the −2126 transcript start site) or 1 hour (for identification of the −1923 and −3041 transcript start sites) for total RNA and cDNA preparation. For the GFP expression experiment (Figures 7, S6 and S7) strains were grown overnight in YNB minimal medium at 30°C, diluted into fresh YNB minimal medium the next day, and grown for 3 hours at 30°C, as described by Wolyniak and Sundstrom (Wolyniak & Sundstrom, 2007); CAF2-1 was used as the wild-type control strain. For the Ume6-Myc expression experiment (Figure 6) strains were grown overnight in YEPD at 30°C and diluted 1:10 into the indicated pre-warmed media. Cells for the 0 hr. time point sample of this experiment were harvested immediately prior to dilution.

RNA Preparation and Analysis

Total RNA preparation and Northern analysis were performed as described previously (Banerjee et al., 2008). Primers used for Northern probes are described in Table S2. RNA from the polysome profiling experiments was extracted with 1:1 phenol:chloroform, precipitated overnight at −20°C with 2 volumes of 70% ethanol in 2.5M LiCl, washed with 70% ethanol and resuspended in nuclease-free water prior to qRT-PCR analysis (del Prete *et al.*, 2007). RNA for qRT-PCR analysis and for 5′ RACE analysis was prepared using the SV Total RNA Isolation Kit (Promega) according to the manufacturer's directions with the following modification: cells were resuspended in 225 μL buffer RLT and placed in a bead beater for 2.5 minutes (yeast) or 5 minutes (hyphae); cells were rested on ice for 1 minute per every 2.5 minutes in the bead beater.

5′ RACE Analysis

5′ RACE analysis was performed using an Ambion FirstChoice® RLM-RACE kit (Applied Biosystems). Briefly, total RNA was first treated with calf intestinal phosphatase (CIP) to remove 5′ phosphates from rRNA, tRNA, degraded mRNA and genomic DNA. Next, the RNA was treated with tobacco acid pyrophosphatase (TAP) to remove cap structures from the full-length mRNAs. A 45 bp 5′ RACE adaptor was then ligated to the decapped mRNA. Following a random-primed reverse transcription reaction, the 5′ end of the *UME6* transcript was then amplified by nested PCR. All 5′ RACE PCR products were run on 0.8% agarose gels and directly sequenced to determine size and identity.

Real-time Quantitative RT-PCR Analysis

cDNA for qRT-PCR analysis was prepared from 2 μg of total RNA treated with DNAse I (Invitrogen) using an Applied Biosystems – High Capacity cDNA Reverse Transcription Kit, according to the manufacturer's instructions. Real-time PCR was performed in duplicate in 96-well plates using the Chromo4 Four-Color Real-Time PCR Detection System (Bio-Rad). PCR reactions were carried out in 25 μL volumes containing 5 μL 1:25 diluted cDNA (original cDNA volume was 20 μL), 12.5 μL GoTaq qPCR Master Mix (Promega) and 4.3 μL dH_2O. Primers used for qRT-PCR analysis are described in Table S2. Real-time PCR was performed using the following cycling conditions: Step 1: 95 °C for 2 minutes, Step 2: 95 °C for 30 seconds, Step 3: annealing temperature (determined for each primer pair) for 1 minute, Step 4: read plate, Step 5: repeat steps 2-4 for 39 times, Step 6: 72 °C for 5 minutes, Step 7: Melting Curve 50 °C – 95 °C every 0.4 °C, hold 1 second and read plate. Standard curves were generated using 7 serial dilutions of a pool of cDNA from each experiment to determine primer efficiency. Expression levels of each gene were normalized to levels of an internal *ACT1* control using the Pfaffl method (Pfaffl, 2001). For the polysome profiling experiment, spike-in mRNA (Solaris) was added to each sample at a final concentration of 1X prior to RNA isolation and expression levels of *UME6* were normalized to spike-in mRNA using the Pfaffl method.

Polysome Profiling Analysis

Cells were treated with 0.1 mg mL^{-1} cycloheximide and incubated on ice for 5 min. Next, cells were washed twice in lysis buffer (20 mM Tris-Cl, pH 8.0, 140 mM KCl, 1.5 mM $MgCl_2$, 0.5 mM DTT, 1% Triton X-100, 0.1 mg mL^{-1} cycloheximide, 1 mg mL^{-1} heparin), lysed by vortexing with 2/3 volume beads for 4 × 20 seconds and centrifuged 5 minutes at 4500 rpm at 4°C. Fifty OD_{260} units of supernatant were loaded on the top of a 10-50% continuous sucrose gradient and centrifuged at 35,000 rpm for 160 minutes at 4°C in a SW41 rotor (Beckman Coulter). Fractions were collected manually in 1 mL aliquots for RNA isolation or 200 μL aliquots to monitor OD_{254} absorbance. RNA was isolated from each fraction for qRT-PCR analysis. For the EDTA release assay, following treatment with 0.1 mg mL^{-1} cycloheximide, 25 mM EDTA was added to the lysis buffer and sucrose gradient.

Western Analysis

Protein isolation was performed as described previously (Cao *et al.*, 2006). 20 μg of total protein extract was separated by 8% (for Ume6-Myc) or 12% (for Act1) SDS-PAGE and transferred to a PVDF membrane (Invitrogen). Membranes were blocked with 5% milk in 1X PBS with 0.01% Tween-20, incubated with primary antibody for Myc (Cell Signaling Technology #2272) or actin (Sigma #A5060) overnight at 4°C, washed three times in 1 × PBS with 0.01% Tween-20, then incubated with HRP-conjugated goat anti-rabbit secondary antibody (Zymed). The ECL system (GE Healthcare) was used for detection. Densitometry quantitation of Western blots was performed using GelQuant.NET software provided by biochemlabsolutions.com.

Fluorometry

Cellular fluorescence levels were quantified as described previously (Wolyniak & Sundstrom, 2007) using COSTAR 96-well plates and a Biotek Synergy 2 microplate reader. Plate wells contained 1.25×10^7 cells of each strain. Fluorometry assays were performed in biological triplicate and technical duplicate. Fluorescence values for each sample were normalized to cell density as determine by OD_{600}.

Supplementary Material

Refer to Web version on PubMed Central for supplementary material.

Acknowledgments

We thank Brian Wickes and other members of the San Antonio Center for Medical Mycology for fruitful discussions and advice during the course of the experiments and for useful comments and suggestions on this manuscript. We especially thank Terri Kinzy (Rutgers Robert Wood Johnson Medical School) as well as Chris Browne and Andrew Link (Vanderbilt University Medical Center) for useful comments and suggestions regarding the polysome profiling analysis. We are grateful to Alistair Brown (University of Aberdeen, United Kingdom), Hironobu Nakayama and Mikio Arisawa (Nippon Roche Research Center, Kamakura, Japan), James Konopka (Stony Brook University) and Haoping Liu (University of California, Irvine) for plasmids and/or strains. We also thank Ian Morris for assistance with statistical analysis and microscopy and Haoping Liu and Yang Lu for assistance and advice with Western analysis. D.S.C. was supported by a COSTAR training grant (National Institute of Dental and Craniofacial Research Grant T32DE14318) as well as a Ruth L. Kirschstein National Research Service Award for Individual Predoctoral Fellows (National Institute of Dental and Craniofacial Research Grant F31DE021930). D.K. was supported by National Institute of Allergy and Infectious Diseases Grant 5RO1AI083344 in addition to a Voelcker Young Investigator Award from the Max and Minnie Tomerlin Voelcker Fund. The content is solely the responsibility of the authors and does not necessarily represent the official views of the National Institute of Allergy and Infectious Diseases, the National Institute of Dental and Craniofacial Research or the National Institute of Health.

REFERENCES

Adeli K. Translational control mechanisms in metabolic regulation: critical role of RNA binding proteins, microRNAs, and cytoplasmic RNA granules. Am J Physiol Endocrinol Metab. 2011; 301:E1051–1064. [PubMed: 21971522]

Bachewich C, Whiteway M. Cyclin Cln3p links G1 progression to hyphal and pseudohyphal development in *Candida albicans*. Eukaryot Cell. 2005; 4:95–102. [PubMed: 15643065]

Balvay L, Soto Rifo R, Ricci EP, Decimo D, Ohlmann T. Structural and functional diversity of viral IRESes. Biochimica et biophysica acta. 2009; 1789:542–557. [PubMed: 19632368]

Banerjee M, Thompson DS, Lazzell A, Carlisle PL, Pierce C, Monteagudo C, Lopez-Ribot JL, Kadosh D. *UME6*, a novel filament-specific regulator of *Candida albicans* hyphal extension and virulence. Molecular biology of the cell. 2008; 19:1354–1365. [PubMed: 18216277]

Bassilana M, Blyth J, Arkowitz RA. Cdc24, the GDP-GTP exchange factor for Cdc42, is required for invasive hyphal growth of *Candida albicans*. Eukaryot Cell. 2003; 2:9–18. [PubMed: 12582118]

Bensen ES, Clemente-Blanco A, Finley KR, Correa-Bordes J, Berman J. The mitotic cyclins Clb2p and Clb4p affect morphogenesis in *Candida albicans*. Molecular biology of the cell. 2005; 16:3387–3400. [PubMed: 15888543]

Bensen ES, Filler SG, Berman J. A forkhead transcription factor is important for true hyphal as well as yeast morphogenesis in *Candida albicans*. Eukaryot Cell. 2002; 1:787–798. [PubMed: 12455696]

Biswas S, Van Dijck P, Datta A. Environmental sensing and signal transduction pathways regulating morphopathogenic determinants of *Candida albicans*. Microbiol Mol Biol Rev. 2007; 71:348–376. [PubMed: 17554048]

Braun BR, Johnson AD. Control of filament formation in *Candida albicans* by the transcriptional repressor. TUP1 Science. 1997; 277:105–109.

Braun BR, van Het Hoog M, d'Enfert C, Martchenko M, Dungan J, Kuo A, Inglis DO, Uhl MA, Hogues H, Berriman M, Lorenz M, Levitin A, Oberholzer U, Bachewich C, Harcus D, Marcil A, Dignard D, Iouk T, Zito R, Frangeul L, Tekaia F, Rutherford K, Wang E, Munro CA, Bates S, Gow NA, Hoyer LL, Kohler G, Morschhauser J, Newport G, Znaidi S, Raymond M, Turcotte B, Sherlock G, Costanzo M, Ihmels J, Berman J, Sanglard D, Agabian N, Mitchell AP, Johnson AD, Whiteway M, Nantel A. A human-curated annotation of the *Candida albicans* genome. PLoS genetics. 2005; 1:36–57. [PubMed: 16103911]

Brown DH Jr. Giusani AD, Chen X, Kumamoto CA. Filamentous growth of *Candida albicans* in response to physical environmental cues and its regulation by the unique *CZF1* gene. Molecular microbiology. 1999; 34:651–662. [PubMed: 10564506]

Bruno VM, Wang Z, Marjani SL, Euskirchen GM, Martin J, Sherlock G, Snyder M. Comprehensive annotation of the transcriptome of the human fungal pathogen *Candida albicans* using RNA-seq. Genome Res. 2010; 20:1451–1458. [PubMed: 20810668]

Calderone, RA.; Clancy, CJ. *Candida* and Candidiasis. ASM Press; Washington, D.C.: 2012.

Cameron AD, Volar M, Bannister LA, Redfield RJ. RNA secondary structure regulates the translation of sxy and competence development in *Haemophilus influenzae*. Nucleic acids research. 2008; 36:10–20. [PubMed: 17981840]

Cao F, Lane S, Raniga PP, Lu Y, Zhou Z, Ramon K, Chen J, Liu H. The Flo8 transcription factor is essential for hyphal development and virulence in *Candida albicans*. Molecular biology of the cell. 2006; 17:295–307. [PubMed: 16267276]

Carlisle PL, Banerjee M, Lazzell A, Monteagudo C, Lopez-Ribot JL, Kadosh D. Expression levels of a filament-specific transcriptional regulator are sufficient to determine *Candida albicans* morphology and virulence. Proceedings of the National Academy of Sciences of the United States of America. 2009; 106:599–604. [PubMed: 19116272]

Carlisle PL, Kadosh D. *Candida albicans* Ume6, a filament-specific transcriptional regulator, directs hyphal growth via a pathway involving Hgc1 cyclin-related protein. Eukaryot Cell. 2010; 9:1320–1328. [PubMed: 20656912]

Chapa y Lazo B, Bates S, Sudbery P. The G1 cyclin Cln3 regulates morphogenesis in *Candida albicans*. Eukaryot Cell. 2005; 4:90–94. [PubMed: 15643064]

Chatterjee S, Pal JK. Role of 5′- and 3′-untranslated regions of mRNAs in human diseases. Biol Cell. 2009; 101:251–262. [PubMed: 19275763]

Chen C, Noble SM. Post-transcriptional regulation of the Sef1 transcription factor controls the virulence of *Candida albicans* in its mammalian host. PLoS pathogens. 2012; 8:e1002956. [PubMed: 23133381]

Chen C, Pande K, French SD, Tuch BB, Noble SM. An iron homeostasis regulatory circuit with reciprocal roles in *Candida albicans* commensalism and pathogenesis. Cell host & microbe. 2011; 10:118–135. [PubMed: 21843869]

Chen J, Rappsilber J, Chiang YC, Russell P, Mann M, Denis CL. Purification and characterization of the 1.0 MDa CCR4-NOT complex identifies two novel components of the complex. Journal of molecular biology. 2001; 314:683–694. [PubMed: 11733989]

Cleary IA, Lazzell AL, Monteagudo C, Thomas DP, Saville SP. *BRG1* and *NRG1* form a novel feedback circuit regulating *Candida albicans* hypha formation and virulence. Molecular microbiology. 2012; 85:557–573. [PubMed: 22757963]

Dagley MJ, Gentle IE, Beilharz TH, Pettolino FA, Djordjevic JT, Lo TL, Uwamahoro N, Rupasinghe T, Tull DL, McConville M, Beaurepaire C, Nantel A, Lithgow T, Mitchell AP, Traven A. Cell wall integrity is linked to mitochondria and phospholipid homeostasis in *Candida albicans* through the activity of the post-transcriptional regulator Ccr4-Pop2. Molecular microbiology. 2011; 79:968–989. [PubMed: 21299651]

Davuluri RV, Suzuki Y, Sugano S, Zhang MQ. CART classification of human 5′ UTR sequences. Genome Res. 2000; 10:1807–1816. [PubMed: 11076865]

del Prete MJ, Vernal R, Dolznig H, Mullner EW, Garcia-Sanz JA. Isolation of polysome-bound mRNA from solid tissues amenable for RT-PCR and profiling experiments. Rna. 2007; 13:414–421. [PubMed: 17237355]

Douglas LJ. Medical importance of biofilms in *Candida* infections. Rev Iberoam Micol. 2002; 19:139–143. [PubMed: 12825991]

Dupont PF. *Candida albicans*, the opportunist. A cellular and molecular perspective. J Am Podiatr Med Assoc. 1995; 85:104–115. [PubMed: 7877106]

Edmond MB, Wallace SE, McClish DK, Pfaller MA, Jones RN, Wenzel RP. Nosocomial bloodstream infections in United States hospitals: a three-year analysis. Clin Infect Dis. 1999; 29:239–244. [PubMed: 10476719]

Elson SL, Noble SM, Solis NV, Filler SG, Johnson AD. An RNA transport system in *Candida albicans* regulates hyphal morphology and invasive growth. PLoS genetics. 2009; 5:e1000664. [PubMed: 19779551]

Felk A, Kretschmar M, Albrecht A, Schaller M, Beinhauer S, Nichterlein T, Sanglard D, Korting HC, Schafer W, Hube B. *Candida albicans* hyphal formation and the expression of the Efg1-regulated proteinases Sap4 to Sap6 are required for the invasion of parenchymal organs. Infection and immunity. 2002; 70:3689–3700. [PubMed: 12065511]

Frohner IE, Bourgeois C, Yatsyk K, Majer O, Kuchler K. *Candida albicans* cell surface superoxide dismutases degrade host-derived reactive oxygen species to escape innate immune surveillance. Molecular microbiology. 2009; 71:240–252. [PubMed: 19019164]

Grillo G, Turi A, Licciulli F, Mignone F, Liuni S, Banfi S, Gennarino VA, Horner DS, Pavesi G, Picardi E, Pesole G. UTRdb and UTRsite (RELEASE 2010): a collection of sequences and regulatory motifs of the untranslated regions of eukaryotic mRNAs. Nucleic acids research. 2010; 38:D75–80. [PubMed: 19880380]

Guida A, Lindstadt C, Maguire SL, Ding C, Higgins DG, Corton NJ, Berriman M, Butler G. Using RNA-seq to determine the transcriptional landscape and the hypoxic response of the pathogenic yeast *Candida parapsilosis*. BMC genomics. 2011; 12:628. [PubMed: 22192698]

Hnisz D, Majer O, Frohner IE, Komnenovic V, Kuchler K. The Set3/Hos2 histone deacetylase complex attenuates cAMP/PKA signaling to regulate morphogenesis and virulence of *Candida albicans*. PLoS pathogens. 2010; 6:e1000889. [PubMed: 20485517]

Hoyer LL. The *ALS* gene family of *Candida albicans*. Trends Microbiol. 2001; 9:176–180. [PubMed: 11286882]

Hoyer LL, Green CB, Oh SH, Zhao X. Discovering the secrets of the *Candida albicans* agglutinin-like sequence (ALS) gene family--a sticky pursuit. Medical mycology. 2008; 46:1–15. [PubMed: 17852717]

Hube B, Stehr F, Bossenz M, Mazur A, Kretschmar M, Schafer W. Secreted lipases of *Candida albicans*: cloning, characterisation and expression analysis of a new gene family with at least ten members. Arch Microbiol. 2000; 174:362–374. [PubMed: 11131027]

Johansson J, Mandin P, Renzoni A, Chiaruttini C, Springer M, Cossart P. An RNA thermosensor controls expression of virulence genes in *Listeria monocytogenes*. Cell. 2002; 110:551–561. [PubMed: 12230973]

Jung JH, Kim J. Accumulation of P-bodies in *Candida albicans* under different stress and filamentous growth conditions. Fungal genetics and biology. 2011; 48:1116–1123. [PubMed: 22056521]

Kadosh D, Johnson AD. Rfg1, a protein related to the *Saccharomyces cerevisiae* hypoxic regulator Rox1, controls filamentous growth and virulence in *Candida albicans*. Molecular and cellular biology. 2001; 21:2496–2505. [PubMed: 11259598]

Kadosh D, Johnson AD. Induction of the *Candida albicans* filamentous growth program by relief of transcriptional repression: a genome-wide analysis. Molecular biology of the cell. 2005; 16:2903–2912. [PubMed: 15814840]

Kozak M. Circumstances and mechanisms of inhibition of translation by secondary structure in eucaryotic mRNAs. Molecular and cellular biology. 1989; 9:5134–5142. [PubMed: 2601712]

Kozak M. New ways of initiating translation in eukaryotes? Molecular and cellular biology. 2001; 21:1899–1907. [PubMed: 11238926]

Kumamoto CA, Vinces MD. Contributions of hyphae and hypha-co-regulated genes to *Candida albicans* virulence. Cell Microbiol. 2005; 7:1546–1554. [PubMed: 16207242]

Leach MD, Brown AJ. Posttranslational modifications of proteins in the pathobiology of medically relevant fungi. Eukaryot Cell. 2012; 11:98–108. [PubMed: 22158711]

Leach MD, Stead DA, Argo E, Brown AJ. Identification of sumoylation targets, combined with inactivation of *SMT3*, reveals the impact of sumoylation upon growth, morphology, and stress resistance in the pathogen *Candida albicans*. Molecular biology of the cell. 2011a; 22:687–702. [PubMed: 21209325]

Leach MD, Stead DA, Argo E, MacCallum DM, Brown AJ. Molecular and proteomic analyses highlight the importance of ubiquitination for the stress resistance, metabolic adaptation, morphogenetic regulation and virulence of *Candida albicans*. Molecular microbiology. 2011b; 79:1574–1593. [PubMed: 21269335]

Lee KL, Buckley HR, Campbell CC. An amino acid liquid synthetic medium for the development of mycelial and yeast forms of *Candida albicans*. Sabouraudia. 1975; 13:148–153. [PubMed: 808868]

Li Y, Su C, Mao X, Cao F, Chen J. Roles of *Candida albicans* Sfl1 in hyphal development. Eukaryot Cell. 2007; 6:2112–2121. [PubMed: 17715361]

Liu H, Kohler J, Fink GR. Suppression of hyphal formation in *Candida albicans* by mutation of a *STE12* homolog. Science. 1994; 266:1723–1726. [PubMed: 7992058]

Lo HJ, Kohler JR, DiDomenico B, Loebenberg D, Cacciapuoti A, Fink GR. Nonfilamentous *C. albicans* mutants are avirulent. Cell. 1997; 90:939–949. [PubMed: 9298905]

Lopes da Rosa J, Boyartchuk VL, Zhu LJ, Kaufman PD. Histone acetyltransferase Rtt109 is required for *Candida albicans* pathogenesis. Proceedings of the National Academy of Sciences of the United States of America. 2010; 107:1594–1599. [PubMed: 20080646]

Lopes da Rosa J, Kaufman PD. Chromatin-mediated *Candida albicans* virulence. Biochimica et biophysica acta. 2012; 1819:349–355. [PubMed: 21888998]

Lu Y, Su C, Solis NV, Filler SG, Liu H. Synergistic Regulation of Hyphal Elongation by Hypoxia, CO_2, and Nutrient Conditions Controls the Virulence of *Candida albicans*. Cell host & microbe. 2013; 14:499–509. [PubMed: 24237696]

Lu Y, Su C, Wang A, Liu H. Hyphal development in *Candida albicans* requires two temporally linked changes in promoter chromatin for initiation and maintenance. PLoS biology. 2011; 9:e1001105. [PubMed: 21811397]

Martchenko M, Alarco AM, Harcus D, Whiteway M. Superoxide dismutases in *Candida albicans*: transcriptional regulation and functional characterization of the hyphal-induced *SOD5* gene. Molecular biology of the cell. 2004; 15:456–467. [PubMed: 14617819]

Mignone F, Gissi C, Liuni S, Pesole G. Untranslated regions of mRNAs. Genome biology. 2002; 3 REVIEWS0004.

Miller LG, Hajjeh RA, Edwards JE Jr. Estimating the cost of nosocomial candidemia in the United States. Clin Infect Dis. 2001; 32:1110. [PubMed: 11264044]

Nobile CJ, Fox EP, Nett JE, Sorrells TR, Mitrovich QM, Hernday AD, Tuch BB, Andes DR, Johnson AD. A recently evolved transcriptional network controls biofilm development in *Candida albicans*. Cell. 2012; 148:126–138. [PubMed: 22265407]

Odds, FC. Candida and Candidosis. Baillière Tindall; London: 1988. p. 468

Onyewu C, Wormley FL Jr. Perfect JR, Heitman J. The calcineurin target, Crz1, functions in azole tolerance but is not required for virulence of *Candida albicans*. Infection and immunity. 2004; 72:7330–7333. [PubMed: 15557662]

Park YU, Hur H, Ka M, Kim J. Identification of translational regulation target genes during filamentous growth in *Saccharomyces cerevisiae*: regulatory role of Caf20 and Dhh1. Eukaryot Cell. 2006; 5:2120–2127. [PubMed: 17041186]

Pelletier J, Sonenberg N. Insertion mutagenesis to increase secondary structure within the 5′ noncoding region of a eukaryotic mRNA reduces translational efficiency. Cell. 1985; 40:515–526. [PubMed: 2982496]

Perez-Martin J, Uria JA, Johnson AD. Phenotypic switching in *Candida albicans* is controlled by a *SIR2* gene. EMBO J. 1999; 18:2580–2592. [PubMed: 10228170]

Pfaffl MW. A new mathematical model for relative quantification in real-time RT-PCR. Nucleic acids research. 2001; 29:e45. [PubMed: 11328886]

Pickering BM, Willis AE. The implications of structured 5′ untranslated regions on translation and disease. Semin Cell Dev Biol. 2005; 16:39–47. [PubMed: 15659338]

Ramage G, VandeWalle K, Lopez-Ribot J, Wickes B. The filamentation pathway controlled by the Efg1 regulator protein is required for normal biofilm formation and development in *Candida albicans*. FEMS Microbiol Lett. 2002; 214:95. [PubMed: 12204378]

Sanglard D, Coste A, Ferrari S. Antifungal drug resistance mechanisms in fungal pathogens from the perspective of transcriptional gene regulation. FEMS Yeast Res. 2009; 9:1029–1050. [PubMed: 19799636]

Santos M, de Larrinoa IF. Functional characterization of the *Candida albicans CRZ1* gene encoding a calcineurin-regulated transcription factor. Curr Genet. 2005; 48:88–100. [PubMed: 16044281]

Saville SP, Lazzell AL, Monteagudo C, Lopez-Ribot JL. Engineered control of cell morphology *in vivo* reveals distinct roles for yeast and filamentous forms of *Candida albicans* during infection. Eukaryot Cell. 2003; 2:1053–1060. [PubMed: 14555488]

Schaller M, Bein M, Korting HC, Baur S, Hamm G, Monod M, Beinhauer S, Hube B. The secreted aspartyl proteinases Sap1 and Sap2 cause tissue damage in an *in vitro* model of vaginal candidiasis based on reconstituted human vaginal epithelium. Infection and immunity. 2003; 71:3227–3234. [PubMed: 12761103]

Schaller M, Borelli C, Korting HC, Hube B. Hydrolytic enzymes as virulence factors of *Candida albicans*. Mycoses. 2005; 48:365–377. [PubMed: 16262871]

Sellam A, Hogues H, Askew C, Tebbji F, van Het Hoog M, Lavoie H, Kumamoto CA, Whiteway M, Nantel A. Experimental annotation of the human pathogen *Candida albicans* coding and noncoding transcribed regions using high-resolution tiling arrays. Genome biology. 2010; 11:R71. [PubMed: 20618945]

Sellam A, Tebbji F, Whiteway M, Nantel A. A novel role for the transcription factor Cwt1p as a negative regulator of nitrosative stress in *Candida albicans*. PloS one. 2012; 7:e43956. [PubMed: 22952822]

Shapiro RS, Sellam A, Tebbji F, Whiteway M, Nantel A, Cowen LE. Pho85, Pcl1, and Hms1 signaling governs *Candida albicans* morphogenesis induced by high temperature or Hsp90 compromise. Curr Biol. 2012; 22:461–470. [PubMed: 22365851]

Shen A, Higgins DE. The 5′ untranslated region-mediated enhancement of intracellular listeriolysin O production is required for *Listeria monocytogenes* pathogenicity. Molecular microbiology. 2005; 57:1460–1473. [PubMed: 16102013]

Silver PM, Oliver BG, White TC. Role of *Candida albicans* transcription factor Upc2p in drug resistance and sterol metabolism. Eukaryot Cell. 2004; 3:1391–1397. [PubMed: 15590814]

Sohn K, Urban C, Brunner H, Rupp S. *EFG1* is a major regulator of cell wall dynamics in *Candida albicans* as revealed by DNA microarrays. Molecular microbiology. 2003; 47:89–102. [PubMed: 12492856]

Sonneborn A, Tebarth B, Ernst JF. Control of white-opaque phenotypic switching in *Candida albicans* by the Efg1p morphogenetic regulator. Infection and immunity. 1999; 67:4655–4660. [PubMed: 10456912]

Stoldt VR, Sonneborn A, Leuker CE, Ernst JF. Efg1p, an essential regulator of morphogenesis of the human pathogen *Candida albicans*, is a member of a conserved class of bHLH proteins regulating morphogenetic processes in fungi. EMBO J. 1997; 16:1982–1991. [PubMed: 9155024]

Sundstrom P. Adhesins in *Candida albicans*. Current opinion in microbiology. 1999; 2:353–357. [PubMed: 10458989]

Tripathi G, Wiltshire C, Macaskill S, Tournu H, Budge S, Brown AJ. Gcn4 co ordinates morphogenetic and metabolic responses to amino acid starvation in *Candida albicans*. EMBO J. 2002; 21:5448–5456. [PubMed: 12374745]

Tucker M, Valencia-Sanchez MA, Staples RR, Chen J, Denis CL, Parker R. The transcription factor associated Ccr4 and Caf1 proteins are components of the major cytoplasmic mRNA deadenylase in *Saccharomyces cerevisiae*. Cell. 2001; 104:377–386. [PubMed: 11239395]

Vinces MD, Kumamoto CA. The morphogenetic regulator Czf1p is a DNA-binding protein that regulates white opaque switching in *Candida albicans*. Microbiology. 2007; 153:2877–2884. [PubMed: 17768232]

Wang Y. CDKs and the yeast-hyphal decision. Current opinion in microbiology. 2009; 12:644–649. [PubMed: 19837628]

Weig M, Gross U, Muhlschlegel F. Clinical aspects and pathogenesis of *Candida* infection. Trends Microbiol. 1998; 6:468–470. [PubMed: 10036723]

Wisplinghoff H, Bischoff T, Tallent SM, Seifert H, Wenzel RP, Edmond MB. Nosocomial bloodstream infections in US hospitals: analysis of 24,179 cases from a prospective nationwide surveillance study. Clin Infect Dis. 2004; 39:309–317. [PubMed: 15306996]

Wolyniak MJ, Sundstrom P. Role of actin cytoskeletal dynamics in activation of the cyclic AMP pathway and *HWP1* gene expression in *Candida albicans*. Eukaryot Cell. 2007; 6:1824–1840. [PubMed: 17715368]

Wong KK, Bouwer HG, Freitag NE. Evidence implicating the 5′ untranslated region of *Listeria monocytogenes actA* in the regulation of bacterial actin-based motility. Cell Microbiol. 2004; 6:155–166. [PubMed: 14706101]

Zeidler U, Lettner T, Lassnig C, Muller M, Lajko R, Hintner H, Breitenbach M, Bito A. *UME6* is a crucial downstream target of other transcriptional regulators of true hyphal development in *Candida albicans*. FEMS Yeast Res. 2009; 9:126–142. [PubMed: 19054126]

Zheng X, Wang Y, Wang Y. Hgc1, a novel hypha-specific G1 cyclin-related protein regulates *Candida albicans* hyphal morphogenesis. EMBO J. 2004; 23:1845–1856. [PubMed: 15071502]

Zheng XD, Lee RT, Wang YM, Lin QS, Wang Y. Phosphorylation of Rga2, a Cdc42 GAP, by CDK/Hgc1 is crucial for *Candida albicans* hyphal growth. EMBO J. 2007; 26:3760–3769. [PubMed: 17673907]

Zordan RE, Miller MG, Galgoczy DJ, Tuch BB, Johnson AD. Interlocking transcriptional feedback loops control white-opaque switching in *Candida albicans*. PLoS biology. 2007; 5:e256. [PubMed: 17880264]

Zuker M. Mfold web server for nucleic acid folding and hybridization prediction. Nucleic acids research. 2003; 31:3406–3415. [PubMed: 12824337]

Zuker M, Stiegler P. Optimal computer folding of large RNA sequences using thermodynamics and auxiliary information. Nucleic acids research. 1981; 9:133–148. [PubMed: 6163133]

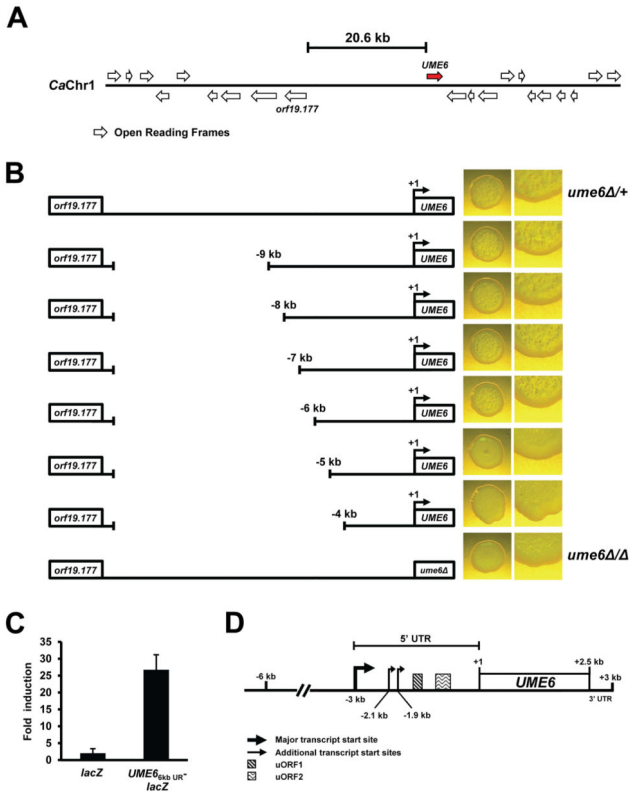

Figure 1.

Characterization of the *UME6* upstream region identifies an exceptionally long 5′ UTR. (A) Schematic representation of the *UME6* locus, and surrounding region, based on *Candida* Genome Database (http://www.candidagenome.org/) annotation (Braun et al., 2005). (B) 3 × 10^3 cells of the indicated strains were spotted on solid YEPD + 10% serum medium, grown at 37°C for 3 days and visualized by light microscopy. Images on the right are enlarged to show spot edges. Please note that only a single *UME6* allele is shown in the schematic representations; the second allele, along with 19.3 kb of the *UME6* upstream intergenic region, has been deleted in all strains except *ume6Δ/Δ*. (C) *C. albicans* strains bearing the indicated reporter constructs were grown overnight in YEPD at 30°C and diluted into pre-warmed YEPD + 10% serum at 37°C (filament-inducing conditions) or YEPD only at 30°C (non-filament-inducing conditions). At 30 minutes post-induction, cells were harvested for total RNA preparation and cDNA synthesis. *lacZ* expression levels were determined by qRT-PCR and normalized to levels of an *ACT1* internal control. Fold induction was determined by dividing normalized *lacZ* values in induced cells by those observed in cells grown under non-filament-inducing conditions. Data shown represents the average of three biological replicates run in technical duplicate (mean ± SEM). (D) Schematic representation of the immediate *UME6* upstream intergenic region (note: not drawn exactly to scale). Transcript start sites were determined by 5′ RACE analysis using cDNA prepared from wild-type (SC5314) cells harvested following induction in YEPD + 10% serum at 37°C.

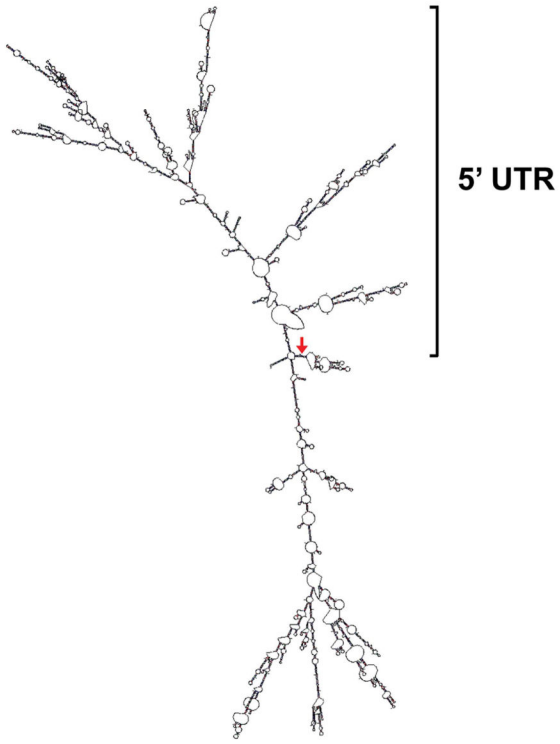

Figure 2.

The *UME6* 5′ UTR is predicted to form a complex and highly stable secondary structure. A predicted structure analysis of the full-length *UME6* transcript sequence, including the 5′ UTR, was performed using Mfold (http://mfold.rna.albany.edu/?q=mfold/), an RNA folding software program that predicts single-stranded RNA minimum folding free energies (Zuker, 2003). The sequence was folded using default parameters (37°C and 1M NaCl) and the predicted secondary structure is shown. Red arrow indicates the translation start site.

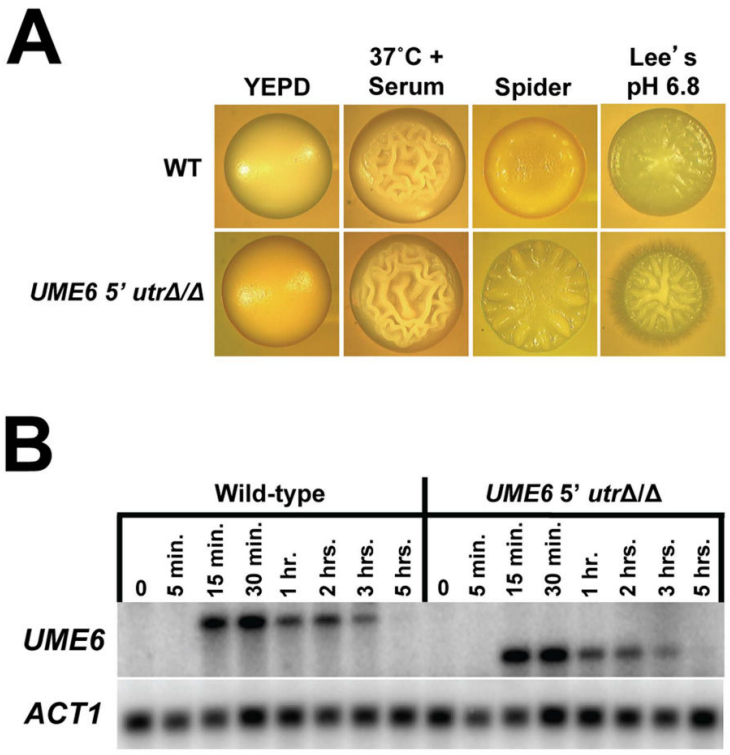

Figure 3.

Deletion of the *UME6* 5′ UTR increases *C. albicans* filamentation but does not affect *UME6* transcript level or induction kinetics. (A) Colony morphologies of the indicated strains grown on solid non-filament-inducing medium (YEPD) or on the indicated solid filament-inducing media. Colonies were grown for 2 days at 30°C on YEPD and Spider media, 2 days at 37°C on YEPD + 10% serum medium, 3 days at 30°C on Lee's pH 6.8 medium and visualized by light microscopy. DK318 was used as the wild-type control strain. (B) The indicated strains were grown in YEPD medium at 30°C and diluted into prewarmed filament-inducing (YEPD + 10% serum at 37°C) medium. Cells were harvested at the indicated time points for total RNA preparation. Northern analysis was performed using 2.5 μg of RNA from each sample and the indicated probes. *ACT1* is included as a loading control. Please note that the *UME6* transcript size is reduced due to deletion of the 5′ UTR.

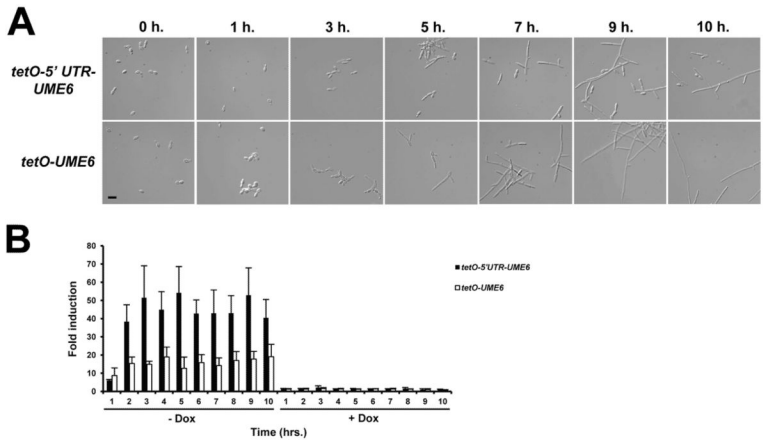

Figure 4.

The 5′ UTR inhibits *UME6*-driven hyphal growth in the absence of filament-inducing conditions but does not cause a reduction in *UME6* transcript levels. (A) The indicated strains were grown overnight in YEPD medium at 30°C in the presence of 1 μg mL^{-1} Dox, washed twice with ddH_2O and inoculated into fresh prewarmed YEPD medium at 30°C in the absence of Dox. Cell aliquots were harvested at the indicated time points, fixed with 4.5% formaldehyde, washed twice with 1X PBS and visualized by DIC microscopy. Bar = 10 μm. (B) Total RNA was isolated from cells grown as described in (A) as well as cells inoculated into fresh prewarmed YEPD medium at 30°C in the presence of 1 μg mL^{-1} Dox as a control. *UME6* transcript levels were determined by qRT-PCR analysis and normalized to those of an *ACT1* internal control. Fold induction was determined by dividing normalized *UME6* expression values for each time point by the normalized *UME6* expression value for the zero time point. Data shown represents the average of three biological replicates run in technical duplicate (mean ± SEM).

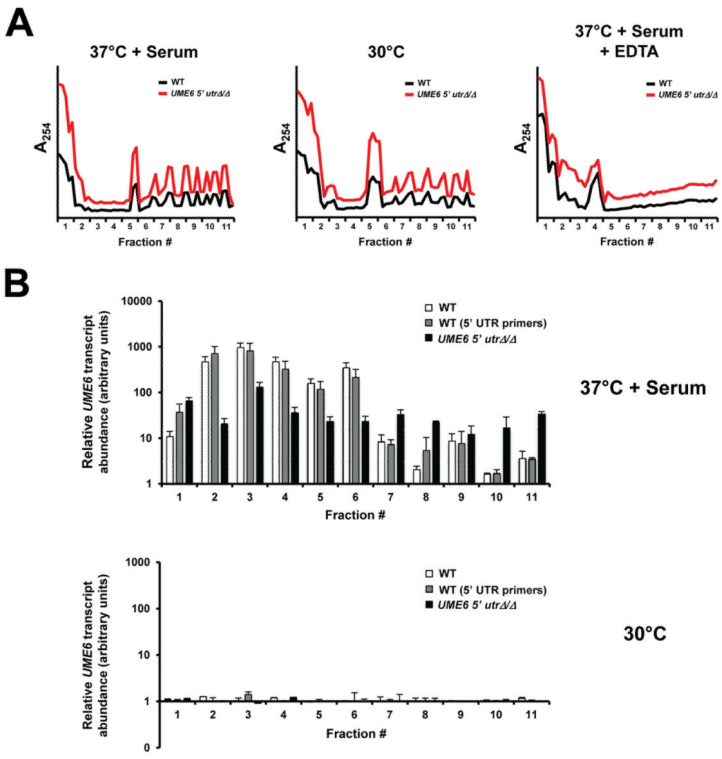

Figure 5.

The *UME6* 5′ UTR functions to inhibit translational efficiency. The indicated strains were grown overnight in YEPD medium at 30°C and diluted into prewarmed YEPD at 30°C (non-filament-inducing conditions) or YEPD + 10% serum at 37°C (filament-inducing conditions). At 30 minutes following serum and temperature induction, cells were treated with 0.1 mg mL^{-1} cycloheximide, lysed (in the presence or absence of 25 mM EDTA for cells grown in YEPD + 10% serum at 37°C), and subjected to sucrose gradient centrifugation for polysome isolation. (A) Polysome profiles across sucrose gradients for the indicated strains grown in YEPD at 30°C or YEPD + 10% serum at 37°C (+/− EDTA treatment) are shown; please note that profiles for each strain are offset. (B) RNA was extracted from each fraction of the indicated sucrose gradients to determine the abundance of *UME6* transcript by qRT-PCR analysis. Data shown represents normalized mean *UME6* transcript levels based on two independent experiments (± SEM). Please note that in the presence of serum at 37°C there is a statistically significant increase in *UME6* transcript abundance in *UME6 5′ utr*Δ/Δ vs. wild-type (WT) strains for the polysome fractions 7,10 and 11 ($p \leq 0.01$ as determined by Student's *t* test).

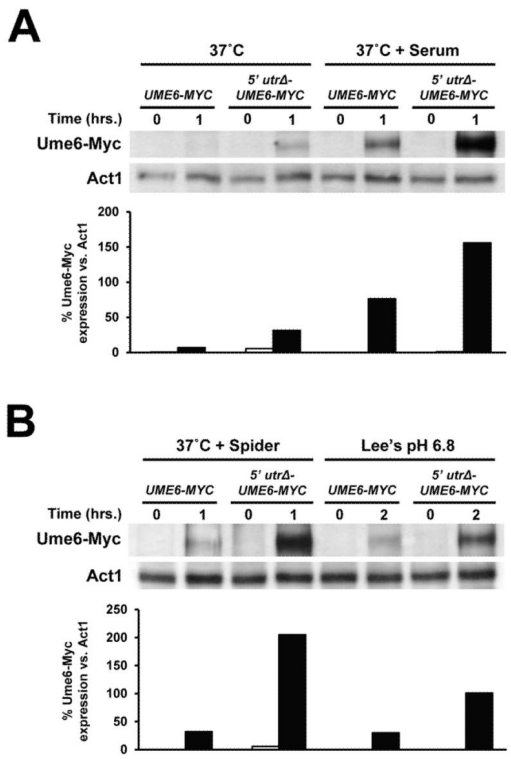

Figure 6.

The *UME6* 5′ UTR inhibits Ume6 protein expression under a variety of filament-inducing conditions. The indicated strains were grown overnight in YEPD at 30°C and diluted 1:100 into pre-warmed YEPD at 37°C (37°C) and YEPD + 10% serum at 37°C (37°C + Serum) (A) or Spider at 37°C (37°C + Spider) and Lee's pH 6.8 medium at 30°C (Lee's pH 6.8) (B). Cells were harvested for protein isolation at the indicated time points and protein levels were determined by Western analysis. Act1 is shown as a loading control. Densitometry quantitation of Ume6-Myc expression vs. Act1 is shown below each respective Western (sample order is the same as that listed for each blot). White bars = 0 hour time point. Black bars = 1 hour time point (or 2 hour time point for the Lee's pH 6.8 condition).

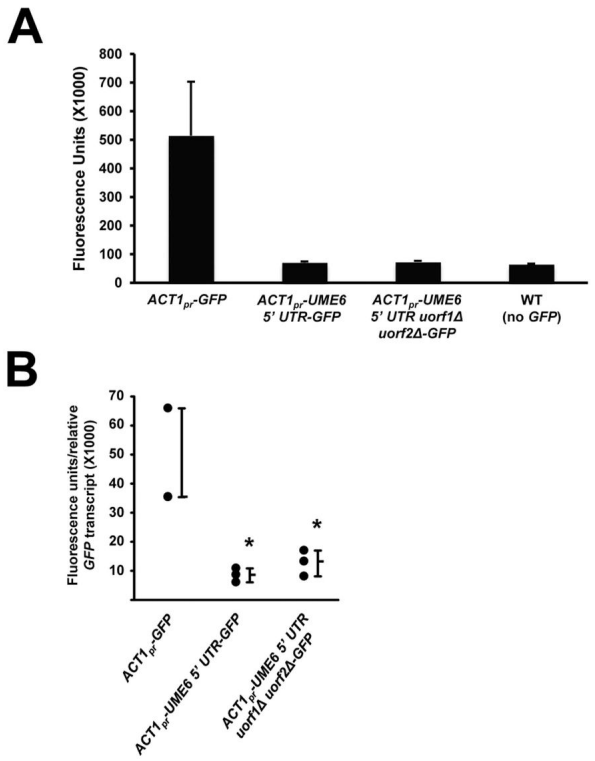

Figure 7.

The *UME6* 5′ UTR is sufficient to inhibit translation of a heterologous *GFP* reporter. (A) Cells of the indicated strains were grown in YNB minimal medium at 30°C. Fluorescence units were determined by dividing the fluorescence value (485 nm excitation, 535 nm emission) by the optical density (600 nm) of each sample. Data shown represents the average of three biological replicates (mean ± SEM). (B) Cells from part (A) were harvested for RNA isolation and *GFP* transcript levels were measured by qRT-PCR. Fluorescence units determined in (A) were normalized to the relative *GFP* expression of each biological replicate. Data shown is for three biological replicates of each strain. Statistical significance was determined by one-way ANOVA analysis. * = $p < 0.01$ compared to $ACT1_{pr}$-*GFP*.

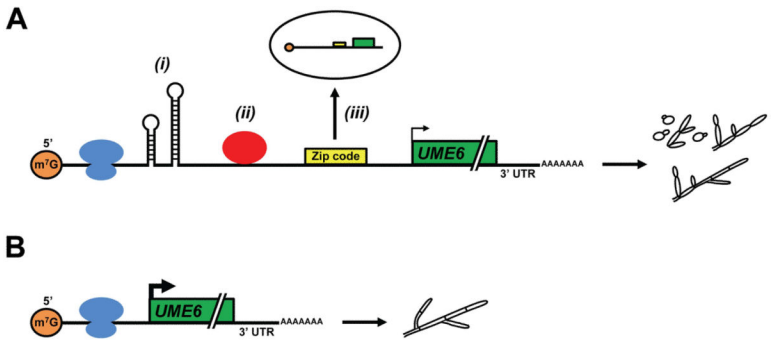

Figure 8.

Model for inhibition of *UME6*-driven hyphal formation in *C. albicans* by the long 5′ UTR. (A) In the presence of the 5′ UTR, scanning and/or access by ribosomes (shown in blue) can be inhibited by the formation of highly stable secondary structures causing a reduction in translational efficiency (i). Translation can also be inhibited by RNA-binding proteins (shown in red) which bind to the 5′ UTR and block access by ribosomes and/or induce formation of secondary structures (ii). Finally, a zip code sequence in the 5′ UTR may direct localization of the *UME6* mRNA to a P-body or other distal cellular compartment (iii). As a consequence of one or more of these mechanisms (they are not mutually exclusive), *UME6* translation will be significantly reduced (small arrow) and cells will form a mixed population of yeast, pseudohyphae and hyphae upon constitutive high-level expression of the *UME6* transcript. (B) In the absence of the long 5′ UTR, translation of *UME6* (large arrow) is not inhibited by any of the mechanisms described above and constitutive high-level *UME6* expression causes cells to form a nearly complete hyphal population. Please note: we cannot exclude the possibility that the 5′ UTR may function to inhibit translation of *UME6* by alternative mechanisms which are not described in part (A).